

† Electronic Supporting Information (ESI)

Electrospun Polarity Controlled Molecular Orientation for Synergistic Performance of Artifact Free Piezoelectric Anisotropic Sensor[†]

Ajay Kumar ^a, Varun Gupta ^a, Pinki Malik ^a, Shanker Ram ^b and Dipankar Mandal ^{a*}

^a Quantum Materials and Devices Unit, Institute of Nano Science and Technology, Knowledge City, Sector 81, Mohali 140306, India

^b Materials Science Centre, Indian Institute of Technology, Kharagpur, 721 302 WB, India

* E-mail: dmandal@inst.ac.in

Discussion D1: Estimating the value of dichroic ratio (R), minimum fraction of completely oriented dipoles (f_m) and range of angle δ formed by their long axis with transition dipole moment vector.^{1,2}

$$R = \frac{\Delta A_{parallel}}{\Delta A_{perpendicular}} \quad (1)$$

$$\text{if } R > 1:0 \cot^{-1}(\sqrt{R}/2); f_m = \frac{R - 1}{R + 2} \quad (2)$$

$$\text{if } R < 1: \cot^{-1}(\frac{\sqrt{R}}{2}) \leq \delta \leq 90^\circ; f_m = \frac{2(1 - R)}{R + 2} \quad (3)$$

Table S1. Variation of the dichroic ratio (R), the minimum fraction of completely oriented dipoles (f_m) and range of angle δ formed by their long axis with transition dipole moment vector for corresponding vibrational modes attached to the wavenumber in positive and negative electrospinning aligned and random fibers of P(VDF-CTFE).³

Fiber	ν (cm ⁻¹)	approximate normal mode assignment	R	f _m	Estimated α interval
PACF	1430	$\delta(\text{CH}_2) - \text{w}(\text{CH}_2)$	0.45	0.447	$71.43^\circ < \alpha < 90^\circ$
PACF	1402	$\text{w}(\text{CH}_2) + \nu_s(\text{CC})$	2.24	0.292	$0^\circ < \alpha < 53.18^\circ$
PACF	1280	$\nu_s(\text{CF}_2) + \nu_s(\text{CC}) + \delta(\text{CCC})$	0.64	0.270	$68.16^\circ < \alpha < 90^\circ$
PACF	1182	$\nu_{\text{as}}(\text{CF}_2) + \rho(\text{CF}_2) + \rho(\text{CH}_2)$	1.02	0.008	$0^\circ < \alpha < 63.16^\circ$
PACF	1073	$\nu_{\text{as}}(\text{CC}) + \text{w}(\text{CF}_2) + \text{w}(\text{CH}_2)$	2.09	0.267	$0^\circ < \alpha < 54.11^\circ$
PACF	883	$\rho(\text{CH}_2) + \nu_{\text{as}}(\text{CF}_2) + \rho(\text{CF}_2)$	0.91	0.061	$64.48^\circ < \alpha < 90^\circ$
PACF	841	$\nu_s(\text{CF}_2) + \nu_s(\text{CC})$	0.78	0.157	$66.15^\circ < \alpha < 90^\circ$
PRCF	1430	$\delta(\text{CH}_2) - \text{w}(\text{CH}_2)$	0.98	0.010	$63.61^\circ < \alpha < 90^\circ$
PRCF	1402	$\text{w}(\text{CH}_2) + \nu_s(\text{CC})$	1.01	0.003	$0^\circ < \alpha < 63.30^\circ$
PRCF	1280	$\nu_s(\text{CF}_2) + \nu_s(\text{CC}) + \delta(\text{CCC})$	0.95	0.033	$64.01^\circ < \alpha < 90^\circ$
PRCF	1182	$\nu_{\text{as}}(\text{CF}_2) + \rho(\text{CF}_2) + \rho(\text{CH}_2)$	0.97	0.018	$63.75^\circ < \alpha < 90^\circ$
PRCF	1073	$\nu_{\text{as}}(\text{CC}) + \text{w}(\text{CF}_2) + \text{w}(\text{CH}_2)$	0.99	0.002	$63.45^\circ < \alpha < 90^\circ$
PRCF	883	$\rho(\text{CH}_2) + \nu_{\text{as}}(\text{CF}_2) + \rho(\text{CF}_2)$	0.95	0.027	$63.90^\circ < \alpha < 90^\circ$
PRCF	841	$\nu_s(\text{CF}_2) + \nu_s(\text{CC})$	0.96	0.021	$63.61^\circ < \alpha < 90^\circ$
NACF	1430	$\delta(\text{CH}_2) - \text{w}(\text{CH}_2)$	0.24	0.679	$76.24^\circ < \alpha < 90^\circ$
NACF	1402	$\text{w}(\text{CH}_2) + \nu_s(\text{CC})$	2.33	0.307	$0^\circ < \alpha < 52.63^\circ$
NACF	1280	$\nu_s(\text{CF}_2) + \nu_s(\text{CC}) + \delta(\text{CCC})$	0.75	0.178	$66.51^\circ < \alpha < 90^\circ$
NACF	1182	$\nu_{\text{as}}(\text{CF}_2) + \rho(\text{CF}_2) + \rho(\text{CH}_2)$	1.04	0.013	$0^\circ < \alpha < 62.99^\circ$
NACF	1073	$\nu_{\text{as}}(\text{CC}) + \text{w}(\text{CF}_2) + \text{w}(\text{CH}_2)$	2.01	0.252	$0^\circ < \alpha < 54.63^\circ$
NACF	883	$\rho(\text{CH}_2) + \nu_{\text{as}}(\text{CF}_2) + \rho(\text{CF}_2)$	0.92	0.052	$64.34^\circ < \alpha < 90^\circ$
NACF	841	$\nu_s(\text{CF}_2) + \nu_s(\text{CC})$	0.93	0.049	$63.57^\circ < \alpha < 90^\circ$
NRCF	1430	$\delta(\text{CH}_2) - \text{w}(\text{CH}_2)$	0.98	0.008	$64.28^\circ < \alpha < 90^\circ$
NRCF	1402	$\text{w}(\text{CH}_2) + \nu_s(\text{CC})$	0.92	0.056	$64.40^\circ < \alpha < 90^\circ$
NRCF	1280	$\nu_s(\text{CF}_2) + \nu_s(\text{CC}) + \delta(\text{CCC})$	1.02	0.007	$0^\circ < \alpha < 63.52^\circ$
NRCF	1182	$\nu_{\text{as}}(\text{CF}_2) + \rho(\text{CF}_2) + \rho(\text{CH}_2)$	0.99	0.005	$63.43^\circ < \alpha < 90^\circ$
NRCF	1073	$\nu_{\text{as}}(\text{CC}) + \text{w}(\text{CF}_2) + \text{w}(\text{CH}_2)$	0.91	0.058	$63.35^\circ < \alpha < 90^\circ$
NRCF	883	$\rho(\text{CH}_2) + \nu_{\text{as}}(\text{CF}_2) + \rho(\text{CF}_2)$	1.01	0.002	$0^\circ < \alpha < 63.55^\circ$
NRCF	841	$\nu_s(\text{CF}_2) + \nu_s(\text{CC})$	0.98	0.007	$63.57^\circ < \alpha < 90^\circ$

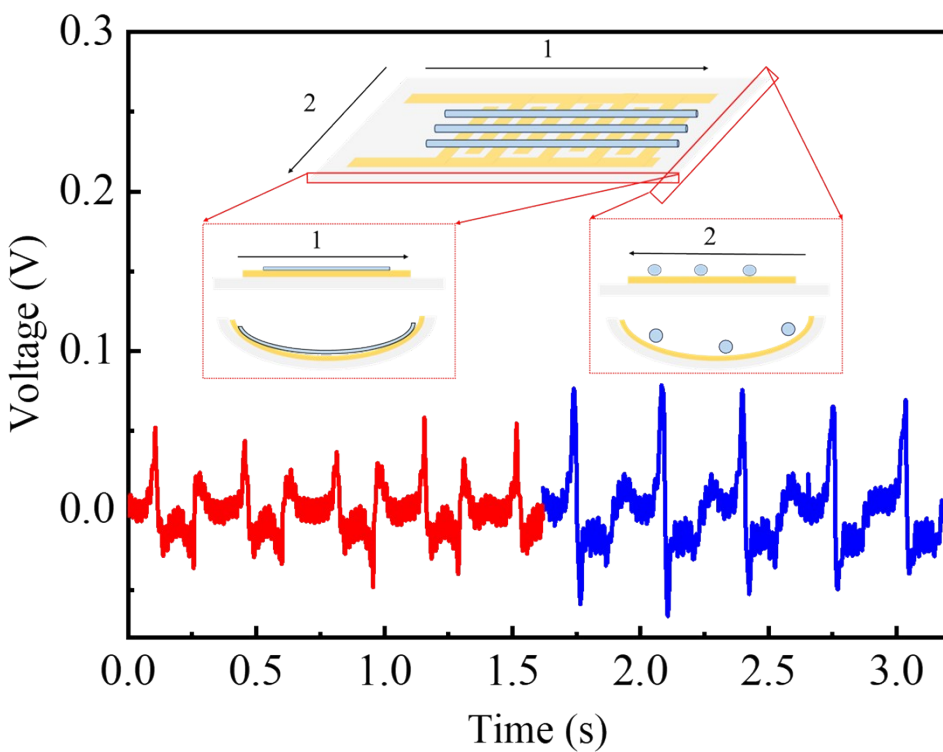


Figure S1. Voltage vs time response under different bending modes (bending angle 60°) to investigate the lateral anisotropy with insets describing the corresponding bending along 1 and 2 axes.

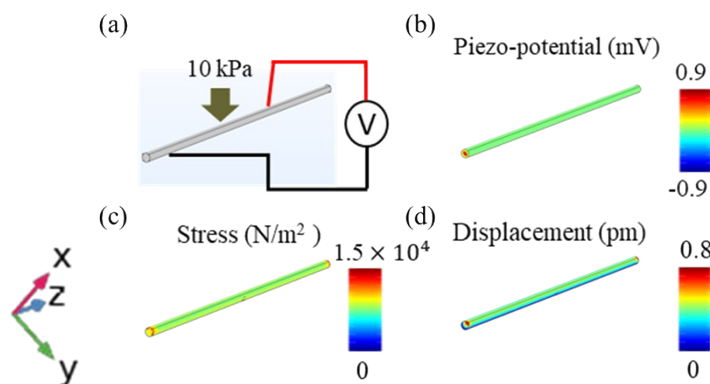


Figure S2. Finite element analysis (a) describing d_{32} mode fiber under stress with corresponding (b) piezo-potential, (c) distribution of stress and (d) displacement generated in the fiber.

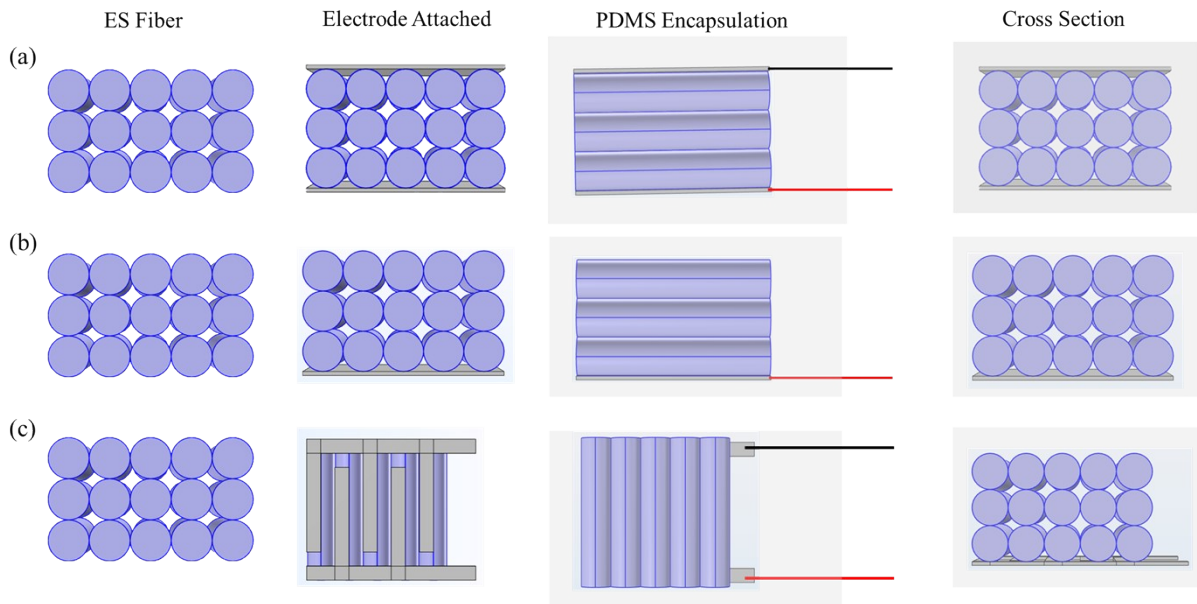


Figure S3. Schematic of the step-wise device fabrication for (a) ferroelectret, (b) triboelectric and (c) piezoelectric signal measurement. In particular, three principal steps of fabrication, viz., ES fiber arrangement, electrode attachment and PDMS encapsulation are shown. In each, the cross-section views are also illustrated to demonstrate three different types of devices, viz., ferroelectret, triboelectric and piezoelectric sensors.

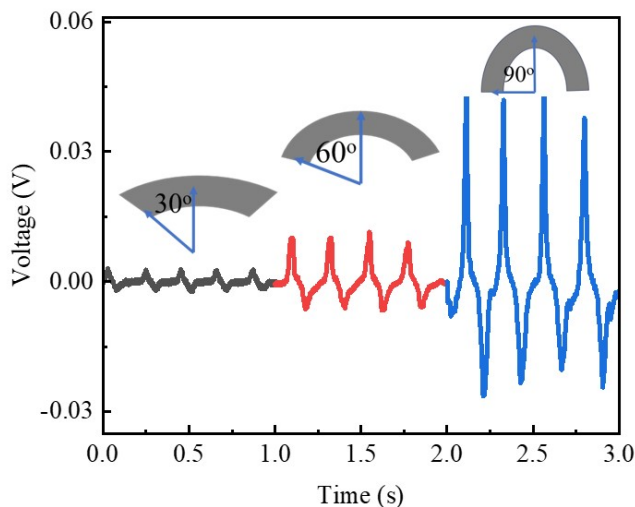


Figure S4. PENG response under different bending angles of 30°, 60° and 90°. The schematics of corresponding bending angles are shown in the inset.

References:

1. Viola, G.; Chang, J.; Maltby, T.; Steckler, F.; Jomaa, M.; Sun, J.; Edusei, J.; Zhang, D.; Vilches, A.; Gao, S.; Liu, X.; Saeed, S.; Zabalawi, H.; Gale, J.; Song, W., Bioinspired multiresonant acoustic devices based on electrospun piezoelectric polymeric nanofibers. *ACS Appl. Mater. Interfaces* **2020**, *12*, 34643–34657.
2. Ma, X.; Liu, J.; Ni, C.; Martin, D. C.; Chase, D. B.; Rabolt, J. F., Molecular orientation in electrospun poly(vinylidene fluoride) fibers. *ACS Macro Lett.* **2012**, *1*, 428–431.
3. Wang, Z.; Sun, B.; Lu, X.; Wang, C.; Su, Z., Molecular orientation in individual electrospun nanofibers studied by polarized AFM–IR. *Macromolecules* **2019**, *52*, 9639–9645.